World Academy of Science, Engineering and Technology
International Journal of Aerospace and Mechanical Engineering
Vol:15, No:1, 2021

Triggering Supersonic Boundary-Layer Instability by Small-Scale Vortex Shedding

Guohua Tu, Zhi Fu, Zhiwei Hu, Neil D Sandham, Jianqiang Chen

***Abstract*—**Tripping of boundary-layers from laminar to turbulent flow, which may be necessary in specific practical applications, requires high amplitude disturbances to be introduced into the boundary layers without large drag penalties. As a possible improvement on fixed trip devices, a technique based on vortex shedding for enhancing supersonic flow transition is demonstrated in the present paper for a Mach 1.5 boundary layer. The compressible Navier-Stokes equations are solved directly using a high-order (fifth-order in space and third-order in time) finite difference method for small-scale cylinders suspended transversely near the wall. For cylinders with proper diameter and mount location, asymmetry vortices shed within the boundary layer are capable of tripping laminar-turbulent transition. Full three-dimensional simulations showed that transition was enhanced. A parametric study of the size and mounting location of the cylinder is carried out to identify the most effective setup. It is also found that the vortex shedding can be suppressed by some factors such as wall effect.

***Keywords*—**Boundary layer instability, boundary layer transition, vortex shedding, supersonic flows, flow control.

I. Introduction

FLOW transition can have a significant influence on the lift, drag, stability, and heat transfer properties of air vehicles [1], [2]. Laminar flow is desirable for a requirement of low friction drag design, while laminar-turbulent transition can minimize flow separation, since laminar flows are less able to withstand the adverse pressure gradients that appear in flows with shock-wave/boundary-layer interactions and for vehicles at large angles of attack. Transition via different routes depends on the ingestion and growth of disturbances [3], [4]. The environmental disturbances, after a receptivity process, may undergo eigenmode and/or transient growth, or pass through bypass mechanisms before breakdown to turbulence. It is more of a challenge to understand and control (delay or promote) transition in high speed flow since the process can be slower than in incompressible flow. In the present paper, a method is considered to guarantee effective tripping of a moderately supersonic boundary layer, which may be encountered on a laminar flow transonic wing before the shock interaction.

Roughness has long been used to trigger laminar-turbulent transition, and roughness-induced transition has been extensively investigated through wind tunnels and flight tests. For a wide range of flows, including blunt bodies and lifting-entry vehicles, experimental data for roughness-dominated transition can be correlated with a roughness Reynolds number, $Re_k = u_k k/\nu_k$, defined in terms of the local flow properties at the height k of the roughness element in the undisturbed boundary layer. Von Doenhoff and Braslow [5] reviewed studies on transition with cylindrical elements carried out before 1960s, and gave an empirical criterion for flow transition based on Re_k. However, Schneider [6] found that, although the roughness Reynolds number is useful, it does not come close to correlating all the transition data available. The critical Re_k is influenced by many factors, including the shape of the roughness, the external disturbance level, wall temperature, and flow compressibility [7]-[10]. In supersonic and hypersonic flows, the size of the trip device is usually much larger than that in low speed flows. For example, the trip devices on Hyper X43 and X51 are much large, usually comparable to the local boundary layer thickness, which is several millimeters [11]. Large trip devices can cause loss of total pressure, shock-wave/boundary-layer interactions, heating and drag penalties.

In order to minimize the size of trip device, we need to find an effective way of generating disturbances. A simple passive method of generating boundary layer disturbances is to utilize Kámán-type vortices. It is well known that alternating vortices are shed when the Reynolds number of a circular cylinder (based on the diameter) is larger than 47 in incompressible laminar flows, which means a very tiny cylinder in high-speed flows could generate unsteady vortices. Based on our previous results of 2D simulations [25], this paper further investigates the possibility of generating vortex shedding by a small-scale cylinder, and employing the vortex shedding to enhance instability and boundary layer transition.

II. Numerical Methods and Problem Setup

A. High-Order Numerical Methods

The strong conservative time-dependent Navier-Stokes equations in curvilinear coordinates are marched in time numerically by using an explicit third-order Runge–Kutta method. The formally fifth-order weighted compact nonlinear scheme [12], [13] is applied to the inviscid terms, and the Steger-Warming splitting method [14] is applied to reconstructing inviscid fluxes. Grid metrics, such as $\tilde{\xi}_{x,i+1/2}$, are computed by the conservative metric method of Deng et al. [15]. The viscous terms are discretized by applying the following sixth-order scheme:

Guohua Tu is with the State Key Laboratory of Aerodynamics, China Aerodynamics Research & Development Center, Mianyang, 621000, China (corresponding author, phone: +86-816-2472109, e-mail: ghtu@skla.cardc.cn).

Zhi Fu and Jianqiang Chen are with the Computational Aerodynamics Institute, China Aerodynamics Research & Development Center, Mianyang 621000, China.

Zhiwei Hu and Neil D Sandham are with the Aerodynamics and Flight Mechanics Group, Faculty of Engineering and Environments, University of Southampton, Southampton SO17 1BJ, United Kingdom.

$$\begin{cases} f'_{i+\frac{1}{2}} = \frac{75}{64\Delta x}(f_{i+1} - f_i) - \frac{25}{384\Delta x}(f_{i+2} - f_{i-1}) \\ \qquad + \frac{3}{640\Delta x}(f_{i+3} - f_{i-2}), \\ f''_i = \frac{75}{64\Delta x}\left(f'_{i+\frac{1}{2}} - f'_{i-\frac{1}{2}}\right) - \frac{25}{384\Delta x}\left(f'_{i+\frac{3}{2}} - f'_{i-\frac{3}{2}}\right) \\ \qquad + \frac{3}{640\Delta x}\left(f'_{i+\frac{5}{2}} - f'_{i+\frac{5}{2}}\right). \end{cases} \quad (1)$$

Tu et al. [16] showed that the staggered method of (1), which calculates the cell-edge first derivatives from cell-node variables and then the cell-node second derivatives from the cell-edge first derivatives, can largely reduce numerical oscillations which may appear in the vicinities of discontinuities and in large gradient regions when high-order schemes are used.

A code based on the above high-order methods has been validated through a variety of benchmark cases and applied to many engineering problems [17]-[22]. The validations showed that the code preserves high-order accuracy and has good performance on complex curvilinear grids.

B. Problem Formulation

The aim of the present work is to use a small-scale circular cylinder to generate vortex shedding which can be used to enhance boundary instability. The influence of a suspended cylinder, as sketched in Fig. 1, on the boundary layer stability is investigated.

Fig. 1 Sketches of the problem setups

Simulations are carried out at freestream inflow conditions: $M_\infty = 1.5$, $T_\infty = 202.17$ K, $p_\infty = 18{,}200$ P, and a unit Reynolds number $Re = 1 \times 10^7 \mathrm{m}^{-1}$. Simulations are run for air, which is taken to be thermally perfect with specific heat ratio $\gamma = 1.4$ and Prandtl number $\mathrm{Pr} = 0.72$.

As shown in Fig. 1, a circular cylinder is suspended transversely in the flat plate boundary layer. The gap between the flat plate and the cylinder allows disturbances to propagate upstream. The wall here is nonslip and isothermal with wall temperature $T_w = 293.15$ K, which is equal to the stagnation temperature. Cylinders are tested for diameters ranging from 0.05 mm to 0.6 mm.

In this paper, results are shown in a dimensionless form based on the incoming freestream velocity U^*_∞, density ρ^*_∞, and temperature T^*_∞, and reference time scale $t^*_{Ref} = L^*_{Ref}/U^*_\infty$. Lengths are normalized with a reference length of $L^*_{Ref} = 0.001$ m $= 1$ mm, thus non-dimensional lengths are the same as the dimensional in mm. Variables with a superscript asterisk (*) stand for dimensional quantities. Therefore, the non-dimensional frequency is given by $f = f^* t^*_{Ref}$.

III. Results and Discussions

A local region of absolute instability, leading to global instability, appears for example in flow past a circular cylinder [23], where the well-known Kármán vortex street appears. As shown in Fig. 1, a circular cylinder is suspended transversely in the boundary layer to generate vortex shedding and also to allow fluctuations to propagate upstream through the cylinder-wall gap within the subsonic region of the boundary layer. The cylinder is centered at (x_c, y_c), where $x_c = 40$, while y_c vary from 0.1 to 0.6. The undisturbed boundary thickness at $x = 40$ is 0.372, and the moment thickness is 0.0413. Seven cylinder diameters within the range of $D = 0.05$ to 0.6 are tested. The parameters and coefficients are given in Table I.

TABLE I
Mounting Location, Diameter, Roughness Reynolds Number, Blockage Ratio, and Gap Ratio for the Cylinder

y^*_c (mm)	D^* (mm)	Re_D	$D/\delta_{0.99}$	G/D
0.1	0.05 ~0.1	120.9~241.8	0.134~0.268	1.00~1.50
0.2	0.05 ~0.3	121.1~726.6	0.134~0.807	0.17~3.50
0.3	0.05 ~0.5	430.7~4306.7	0.134~1.345	0.10~5.50
0.4	0.05 ~0.6	500.0~6000.0	0.134~1.613	0.17~7.50
0.5	0.05 ~0.6	500.0~6000.0	0.134~1.613	0.33~9.50
0.6	0.05 ~0.6	500.0~6000.0	0.134~1.613	1.00~11.5

To minimize induced drag and other aerodynamics and thermodynamics penalties, small cylinders are preferred. The current tested cylinder diameter range is practically possible to implement as even the finest cylinder ($D = 0.05$) is an order of magnitude larger than the hot wires that have been used in anemometry. Although the practicalities are not our concern here, it is not unreasonable to suppose that such a wire could be constructed and fixed in position near a wall.

A. Two-Dimensional Simulations

A previous study [25], when the cylinder was centered at $(x_c, y_c) = (40, 0.2)$, and its diameter D = 0.05, 0.1 and 0.2, showed that visible vortex shedding can be observed for the cases with $D = 0.05$ and $D = 0.1$. However, for the cylinder of D = 0.2, the vortex shedding is suppressed. The suppression of vortex shedding is a result of ground effect [24]. As the cylinder diameter increases, the gap between the cylinder and the plate wall decreases, which enhances the ground effect. The gap is not only necessary for vortex shedding, but also allows the acoustic waves to propagate upstream in the subsonic part of the boundary layer.

Simulations are run for two-dimensional (2D) flow with wider range of flow triggering setups. It can be seen from Fig. 2 that when there is vortex shedding from the cylinder, very large fluctuations may appear in the wake of the cylinder. For example, the amplitude of pressure fluctuations (relative to the free stream static pressure) can exceed 20% (Figs. 2 (b), (c) and (e)), and it is believed that the fluctuations have reached a nonlinear saturation status in the 2D flow. By contrast, if the vortices are steady, the fluctuations may disappear (Fig. 2 (a)) or may become acoustic waves (Fig. 2 (f)) with amplitudes

several magnitudes lower than the cases with unsteady vortices (Figs. 2 (b), (c) and (e)).

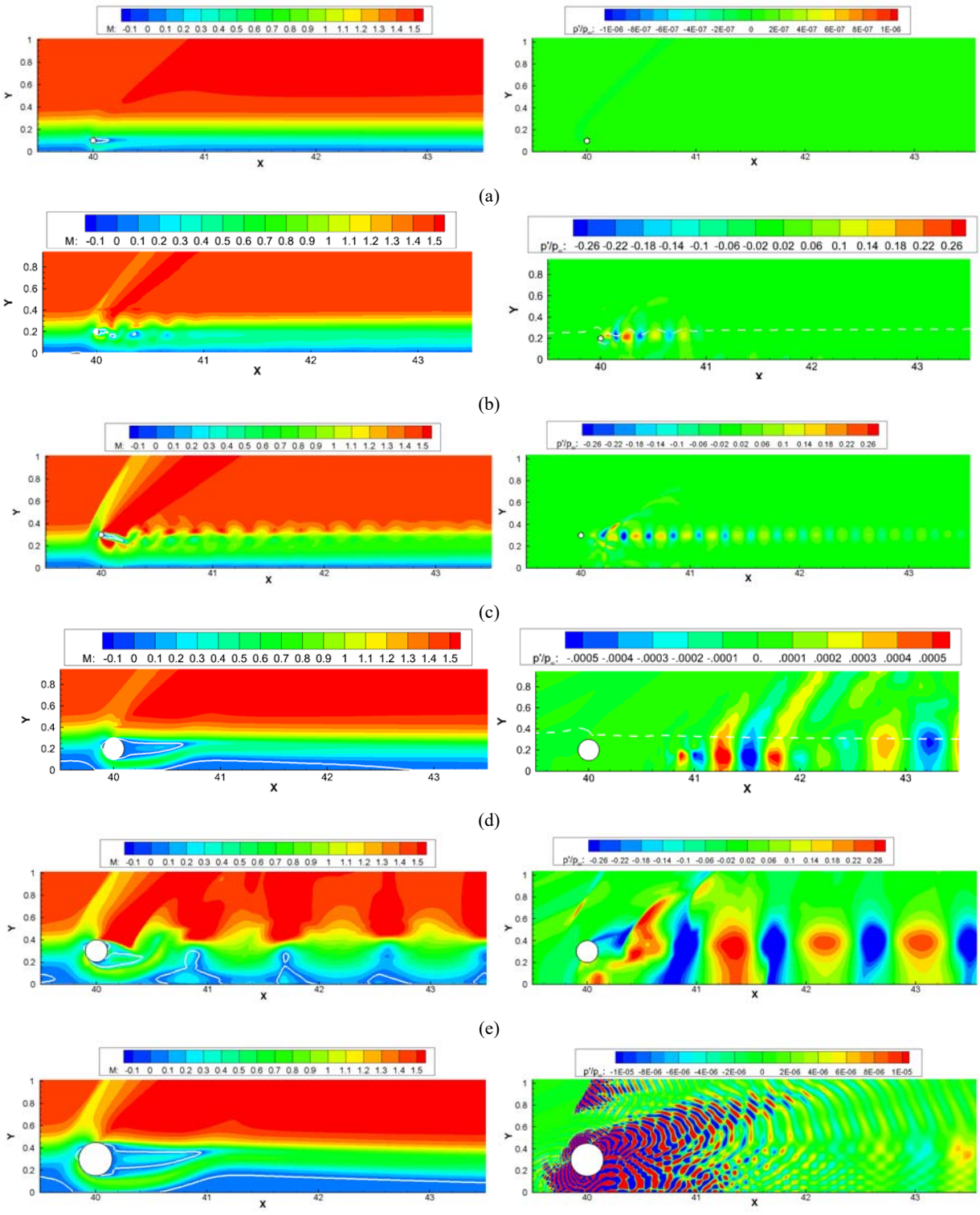

Fig. 2 Snapshots of Mach number M (Left) and pressure fluctuations p'/p_∞ (Right) contours of the flow fields with a cylinder for (a) $D = 0.05$, $y_c = 0.1$; (b) $D = 0.05$, $y_c = 0.2$; (c) $D = 0.05$, $y_c = 0.3$; (d) $D = 0.2$, $y_c = 0.2$; (e) $D = 0.2$, $y_c = 0.3$; (f) $D = 0.3$, $y_c = 0.3$; White solid lines are contours for $u = 0$, and white dashed lines are contours for $M = 1$. The contour levels of the maps in the right column are different

There is also a critical case when $D = 0.2$ for $y_c = 0.2$ (Fig. 2 (d)) where the vortex is marginally unstable but not enough to induce vortex shedding. In this case, the fluctuations do not reach a nonlinear saturation status but are still large enough to cause noticeable disturbances in the boundary layer. Increasing the height of the mounting location (namely y_c) can increase the gap. However, this may induce shock waves if the cylinder is placed in the supersonic region of the boundary layer and may even cause shock-wave/boundary interactions.

The separations in Figs. 2 (a) and (f) are steady. However, there are strong acoustic waves in Fig. 2 (f) while no disturbances in Fig. 2 (a). As shown in Fig. 3, further downstream of the cylinder, the large wavenumber of acoustic waves induces relatively low wavenumber Tollmien–Schlichting (TS) waves. The TS waves are unstable before $x = 49$, but stable again further downstream. The TS waves shown in Fig. 3 are unstable because the cylinder changes the boundary layer profile and induces separations (Fig. 2 (f)). As the boundary layer recovers to its equilibrium state downstream, the TS waves become stable.

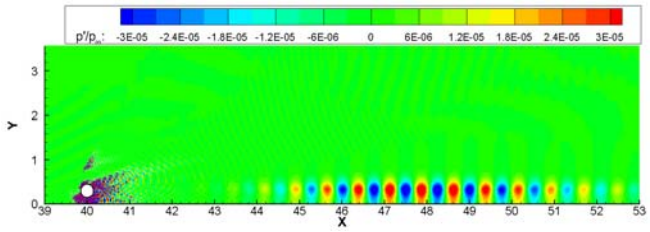

Fig. 3 Pressure fluctuations in the extended domain of the case shown in Fig. 2 (f)

Wall pressure fluctuations are Fourier transformed in time to obtain its power spectral density (PSD). The PSDs show that the non-dimensional frequencies f of fundamental modes are of order $\dot{\cdot}.(1)$ (Please note f^*=4.275$f \times 10^5$Hz). For example, the fundamental mode of the cases with $(x_c, y_c) = (40, 0.2)$, and $D = 0.05$, 0.1, and 0.2 is at frequency $f = 1.834$, 1.070 and $f = 0.734$, respectively. It is worth pointing out that the frequency of the most unstable spatial TS mode of the undisturbed boundary layer at $x = 40$ is 0.0805, and a linear stability analysis shows that the disturbances with frequency higher than 0.12 are stable. We can find that the vortex shedding frequency is much larger than the unstable TS waves. To address the question of whether the vortex shedding can promote laminar-turbulent transition, three-dimensional (3D) simulations have been carried out, which are discussed in the next section. Some wind tunnel experiments will be done in the future.

B. Three-Dimensional Simulations

As the fluctuations may reach nonlinear saturation in 2D simulations and the frequency of the vortex shedding is much higher than the unstable TS waves from a linear stability theory (LST) point of view, it is necessary to investigate the flow in 3D. The setups for the 3D problems are the same as the 2D cases in the *x*-*y* plane, and a spanwise length of 3 millimeters is used with periodic boundary conditions applied in the transverse direction. Fig. 4 shows instantaneous isosurfaces of the second invariant of the velocity gradient tensor (*Q*-criterion). It can be seen that 3D structures appear immediately downstream the cylinder, and lambda vortices appear just about 2 to 3 millimeters downstream of the cylinder (Fig. 4 (a)). The appearance of lambda vortices is usually deemed as an early sign of transition. The lambda vortices are stretched in the streamwise direction and start breaking down at about $x = 50$ (Fig. 4(b)). Fig. 4 (b) indicates that flow becomes fully turbulent at about $x = 60$ ($\mathrm{Re}_x = 6 \times 10^5$).

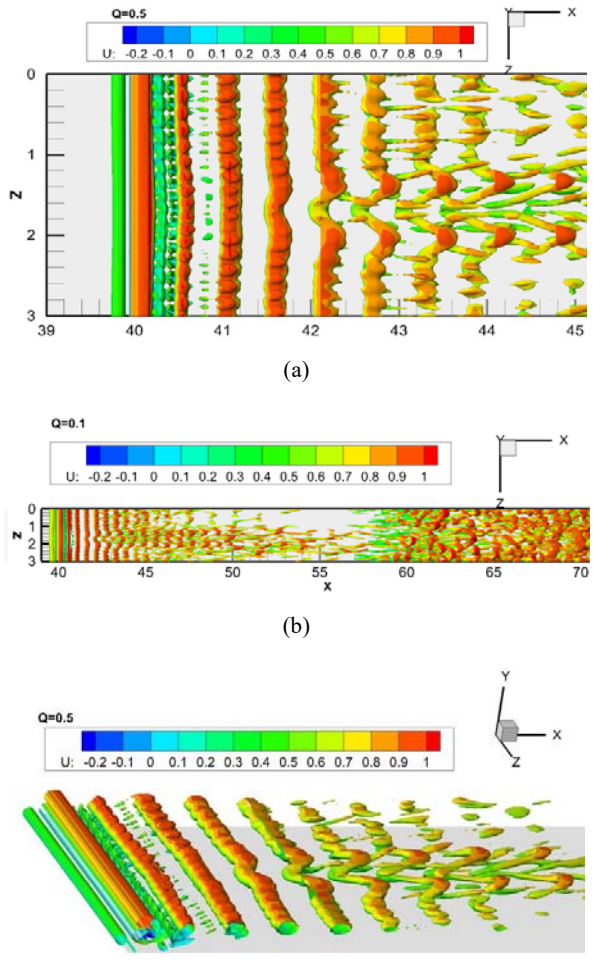

Fig. 4 Three-dimensional simulation of a cylinder centered at $(x_c, y_c) = (40,0.2)$ with diameter of $D = 0.1$; The width of the computational domian is $z = 3$ with periodic boundary conditions. (a) The *Q*=0.5 isosurfaces in the near flow field of the cylinder; (b) The *Q*=0.1 isosurfaces in the extended domain. (c) 3D view of *Q*=0.5 isosurfaces

As shown in the 2D simulations, a cylinder with some parameters may not able to generate large disturbances. In order to enhance instabilities furthermore, we add a rectangular bar downstream of the cylinder (Fig. 5). Our previous 2D simulations show that a feedback loop forms between the cylinder and the bar, and the flow in the feedback loop can be

absolutely and globally unstable [25]. Then, any disturbances in this feedback loop can be amplified. The 3D simulation given in Fig. 6 clearly shows that this feedback loop is capable of enhancing boundary layer instabilities and lambda vortices appear in the near field of the bar (Fig. 6 (a)). The lambda vortices breakdown quickly after they pass over the rectangular bar. In this simulation, we changed the computational domain in the transverse direction to $z = 2.0436$ which is approximately four times the width of the lambda vortex. The extended flow region is shown in Fig. 6 (b).

Fig. 5 The combination of a cylinder and a rectangular bar. Cylinder: $D = 0.1$ and $(x_c, y_c) = (40,0.2)$; Bar: the cross section is rectangular with width of 0.1 and height of 0.2

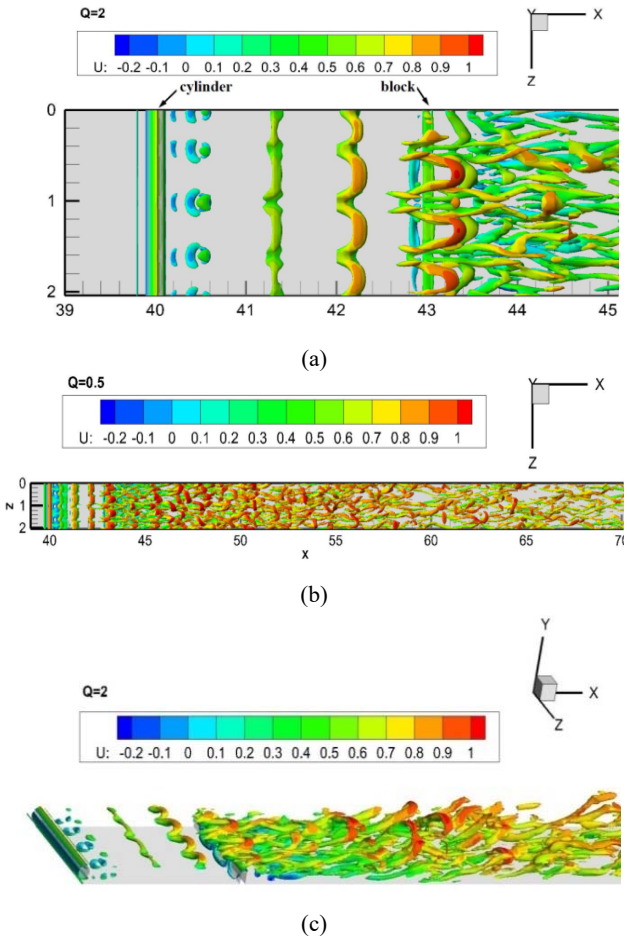

Fig. 6 Three-dimensional simulation of a cylinder-bar combination. The width of the computational domain is $z = 2.0436$ with periodic boundary conditions. (a) The $Q = 2$ isosurfaces in the near flow field of the cylinder; (b) The $Q = 0.5$ isosurfaces in the extended domain. (c) 3D view of Q =2 isosurfaces

From the 3D view of the Q-isosurfaces shown in Figs. 4 (c) and (c), we can find that the stems of the lambda vortices are not on the plate, but in the wake of the cylinder. This phenomenon is consistent to the 2D simulations which show that the strongest fluctuations are in the wake of the cylinders, as indicated in Figs. 2 (b), (c), and (e).

IV. Conclusions

The effect of a suspended small-scale 2D circular cylinder on supersonic boundary layer instability has been investigated numerically by using high-order accurate finite difference schemes. Cylinders of particular diameters were shown to be capable of giving self-excited structures which can enhance boundary layer instabilities. At least two reasons are responsible for the effectiveness of the cylinder. The first one is the vortex shedding which works as a source of adding disturbances. Secondly, the gap between the cylinder and the plate wall allowing the disturbances propagate upstream, which will be receipted by the boundary layer though a receptivity mechanism and then converted downstream to enhance the vortex shedding. The 2D simulations indicate that the gap between the cylinder and the plate wall and the ratio of the gap to the cylinder diameter are critical parameters for producing unsteady vortices. There are thresholds for the existence of vortex shedding. Adding a downstream block (namely bar) can amplify the disturbance, which is very useful in triggering laminar-turbulent transition.

More details, including parameter studies on the cylinder size and its mounting location, the block height and its mounting location, will be included in the final manuscript with the hope of finding some thresholds and critical parameters and some correlations between the parameters and the frequency and strength of the vortex shedding. Also, more details of 3D simulations with further flow field analysis will be finished in the near future.

Acknowledgment

This study was supported by the National Key Research and Development Program of China (Grant 2016YFA0401200). The authors would like to thank Prof. Xunnian Wang and Prof. Qin Li for their help and useful discussions.

References

[1] T .J. Horvath, S. A. Berry, and N. R. Merski, "Hypersonic boundary/shear layer transition for blunt to slender configurations: a NASA Langley experimental perspective," RTO-MP-AVT-111, Art. 22 (2004).
[2] K. D. Fong, X. Wang, and X. Zhong, "Numerical simulation of roughness effect on the stability of a hypersonic boundary layer," Computers & Fluids. 96, 350-367 (2014).
[3] M. V. Morkovin, E. Reshotko, and T. Herbert, "Transition in open flow systems—a reassessment," Bull. Am. Phys. Soc. 39, 1882 (1994)
[4] E. Reshotko, "Transient growth: a factor in bypass transition," Phys. Fluids 13, 1067–1075 (2001).
[5] A. E.Von Doenhoff, and A. L. Braslow, "The effect of distributed surface roughness on laminar flow and flow control," Pergamon Press, Lachmann edition (1961).
[6] S. P. Schneider, "Effects of roughness on hypersonic boundary-layer transition," J. Spacecraft Rockets. 45, 193-209 (2008)
[7] M. Bernardini, S. Pirozzoli, and P. Orlandi, "Compressibility effects on roughness-induced boundary layer transition," International Journal of

Heat and Fluid Flow. 35, 45-51. (2012).
[8] M. A. Kegerise, R. A. King, M. Choudhari, F. Li, and A.T. Norris, "An experimental study of roughness-induced instabilities in a supersonic boundary layer," 7th AIAA Theoretical Fluid Mechanics Conference. AIAA Paper 2014-2501 (2014).
[9] J. A. Redford, N.D. Sandham, and G. T. Roberts, "Numerical simulations of turbulent spots in supersonic boundary layers: effects of Mach number and wall temperature," Progress in Aerospace Sciences, 52, 67-79 (2012).
[10] M. Bernardini, S. Pirozoli, P. Orlandi, and S. K. Lele, "Parameterization of Boundary-Layer Transition Induced by Isolated Roughness Elements" AIAA Journal 52 (10), 2261-2269 (2014).
[11] S. A. Berry, A.H, Auslender, and A.D. Dilley, "Hypersonic boundary-layer trip development for Hyer-X," Journal of Spacecraft and Rocket, 38(6), 853-864 (2001).
[12] X. Deng and H. Zhang, "Developing high-order weighted compact nonlinear schemes," Journal of Computational Physics. 165, 22-44 (2000).
[13] X. Deng, "High-order accurate dissipative weighted compact nonlinear schemes," Science in China Series A: Mathematics. 45, 356-370 (2002).
[14] J. L. Steger and R. F. Warming, "Flux vector splitting of the inviscid gas dynamic equations with application to finite-difference methods," Journal of Computational Physics. 40, 263-293 (1981).
[15] X. Deng, M. Mao, G. Tu, H. Liu, and H. Zhang, "Geometric conservation law and applications to high-order finite difference schemes with stationary grids," Journal of Computational Physics. 230, 1100-1115 (2011).
[16] G. Tu, X. Deng, M. Mao, "A staggered non-oscillatory finite difference method for high-order discretization of viscous terms," Acta Aerodynamica Sinica. 29, 10-15 (2011).
[17] X. Deng, M. Mao, G. Tu, H. Zhang, and Y. Zhang, "High-order and high accurate CFD methods and their applications for complex grid problems," Communication in Computational Physics. 11, 1081-1102 (2012).
[18] X. Deng, M. Mao, G. Tu, Y. Zhang, and H. Zhan, "Extending weighted compact nonlinear schemes to complex grids with characteristic-based interface conditions," AIAA Journal. 48, 2840-2851 (2010).
[19] C. Xu, X. Deng, L. Zhang, J. Fang, G. Wang, Y. Jiang, et al., "Collaborating CPU and GPU for large-scale high-order CFD simulations with complex grids on the TianHe-1A supercomputer," Journal of Computational Physics, 278, 275-297 (2014).
[20] G. Tu, X. Zhao, M. Mao, J. Chen, X. Deng, and H. Liu, "Evaluation of Euler fluxes by a high-order CFD scheme: shock instability," International Journal of Computational Fluid Dynamics. 28, 171-186 (2014).
[21] G. Tu, X. Deng, Y. Min, M. Mao, H. Liu, "Method for evaluating spatial accuracy order of CFD and applications to WCNS scheme on four typically distorted meshes," ACTA Aerodynamica Sinica. 2014, 32, 425-432 (2014).
[22] X. Zhao, G. Tu, H. Liu, M. Mao, and X. Deng, "Applications of WCNS-E-5 in shock-wave/boundary-layer interactions in hypersonic flows," Transactions of Nanjing University of Aeronautics and Astronautics. 30, 81-86 (2013).
[23] P. Huerre and P. A. Monkewitz, "Local and global instabilities in spatially developing flows," Annu. Rev. Fluid Mech. 22, 473-537 (1990).
[24] P. W. Bearman and M. M. Zdravkovich, "Flow around a circular cylinder near a plane boundary," J. Fluid Mech. 89, 33-47 (1978).
[25] G. Tu, Z. Hu, and N. D. Sandham, "Enhanced instability of supersonic boundary layer using passive acoustic feedback," Submitted to Physics of Fluids.